Research Square

Preprints are preliminary reports that have not undergone peer review.
They should not be considered conclusive, used to inform clinical practice,
or referenced by the media as validated information.

NOP10 Directly Interacts with TRAF1 to Activate NF-κB Signalling and Promote Pancreatic Cancer Progression

Jin Dou
The Affiliated Huai'an Hospital of Xuzhou Medical University (The Second People's Hospital of Huai'an)
Jinlong Fan
The Affiliated Huai'an Hospital of Xuzhou Medical University (The Second People's Hospital of Huai'an)
Xiaoyue Wang
The Affiliated Huai'an Hospital of Xuzhou Medical University (The Second People's Hospital of Huai'an)
Mengjie Lv
The Affiliated Huai'an Hospital of Xuzhou Medical University (The Second People's Hospital of Huai'an)
Shan Jiang
The Affiliated Huai'an Hospital of Xuzhou Medical University (The Second People's Hospital of Huai'an)
Haijian Zhao
The Affiliated Huai'an Hospital of Xuzhou Medical University (The Second People's Hospital of Huai'an)
Xiaoyu Zhang
zxy@xzhmu.edu.cn

The Affiliated Huai'an Hospital of Xuzhou Medical University (The Second People's Hospital of Huai'an)

Research Article

Keywords: pancreatic cancer, NOP10, TRAF1, NF-κB, proliferation, prognosis

Posted Date: November 25th, 2026

DOI: https://doi.org/10.21203/rs.3.rs-11797967/v1

License: This work is licensed under a Creative Commons Attribution 4.0 International License.
Read Full License

Additional Declarations: No competing interests reported.

Abstract

Purpose

Pancreatic adenocarcinoma (PAAD) is a highly aggressive malignancy, and constitutive NF-κB activation is a key driver of its progression; however, the upstream mechanisms remain poorly defined. NOP10, a core component of the H/ACA small nucleolar ribonucleoprotein complex, is overexpressed in PAAD and promotes malignant phenotypes, but whether it drives NF-κB signaling through a specific effector is unknown. This study aimed to determine whether NOP10 activates NF-κB through TRAF1 to promote pancreatic cancer progression.

Methods

NOP10 expression and prognosis were analyzed in TCGA-PAAD, GTEx, and GEO datasets. PANC-1 and 8988T cells were subjected to NOP10 knockdown, NOP10 overexpression, and TRAF1 restoration, followed by proliferation, colony formation, wound healing, and Transwell invasion assays, RNA sequencing, and enrichment analyses. Reciprocal co-immunoprecipitation and GST pull-down assays were used to test protein interactions.

Results

NOP10 was upregulated in PAAD tissues and cells and correlated with poor overall survival. Knockdown of NOP10 suppressed proliferation, migration, and invasion, whereas overexpression exerted opposite effects. RNA sequencing identified TRAF1 as a key NOP10-regulated gene. NOP10 positively regulated TRAF1 expression, and the two proteins directly interacted. In PANC-1 cells, TRAF1 restoration reversed NOP10 knockdown-induced downregulation of p-p65 and p50, increased IκBα expression, and rescued proliferation, migration, and invasion.

Conclusion

These results demonstrate that NOP10 directly binds TRAF1 to activate NF-κB signaling, thereby promoting pancreatic cancer progression and providing a potential therapeutic target.

Introduction

Pancreatic adenocarcinoma (PAAD) is among the most aggressive malignancies of the digestive system, characterized by an insidious onset and limited early diagnostic opportunities. Approximately 80% of patients are diagnosed with locally advanced or metastatic disease, and the 5-year survival rate remains below 10% (Stoop et al. 2025; Mannucci and Goel 2026; Blackford et al. 2024). Despite advances in surgical, chemotherapeutic, and radiotherapeutic approaches, drug resistance and disease

recurrence remain major challenges, resulting in a persistently poor prognosis (Jamal and Khan 2025; Li et al. 2025b; Singhal et al. 2024; Ding et al. 2025). Therefore, elucidating the molecular mechanisms underlying PAAD progression and identifying novel therapeutic targets are essential.

NF-κB signalling serves as a central link between inflammation and cancer. In pancreatic cancer, NF-κB is frequently constitutively activated, promoting cell proliferation, suppressing apoptosis, inducing epithelial–mesenchymal transition and angiogenesis, and contributing to tumor progression and chemoresistance (Ding et al. 2025; Li et al. 2026; Zhou et al. 2026; Chen et al. 2025). It also contributes to remodelling of the immunosuppressive tumor microenvironment (Yang et al. 2025; Jenkins et al. 2025; Cao et al. 2025; Tang et al. 2026). However, the upstream mechanisms responsible for sustained NF-κB activation in pancreatic cancer remain incompletely understood.

TRAF1 (TNF receptor-associated factor 1) is an important adaptor protein within the TNFR1 signalling complex. TRAF1 recruits and activates the IKK complex, facilitating IκBα phosphorylation and degradation, releasing p65/p50 dimers for nuclear translocation and NF-κB-dependent transcription (Jang et al. 2024; He et al. 2026). TRAF1 dysregulation has been reported in several cancers, where it contributes to the regulation of cell proliferation, survival, and the tumor immune microenvironment (He et al. 2026; Zhang et al. 2025; Yuan et al. 2025). Thus, identifying upstream regulators of TRAF1 in pancreatic cancer may provide insight into the mechanisms underlying constitutive NF-κB activation.

NOP10 is one of the four core components of the H/ACA small nucleolar ribonucleoprotein (snoRNP) complex and is involved in ribosomal RNA pseudouridylation, ribosome assembly, and telomerase activity maintenance (Ye et al. 2025; Chauhan et al. 2024; Panwar et al. 2025; Ghanim et al. 2024). Emerging evidence indicates that snoRNAs and their associated snoRNP components are dysregulated in various cancers and contribute to tumorigenesis (Ye et al. 2025; Chauhan et al. 2024; Li et al. 2025a; Park et al. 2026; Groza et al. 2026). Our previous study identified NOP10 overexpression in pancreatic cancer and its association with poor prognosis. NOP10 knockdown also suppressed cellular proliferation, migration, invasion, and subcutaneous tumor growth (Dou et al. 2024). However, the downstream mechanisms through which NOP10 promotes pancreatic cancer progression, particularly its involvement in specific signalling pathways, remain unclear.

To investigate these mechanisms, transcriptomic profiling was performed in NOP10-knockdown PANC-1 and 8988T cells, identifying TRAF1 as a key differentially expressed gene (DEG) through cross-cell-line intersection analysis. The positive regulation of TRAF1 by NOP10 was validated, and their protein–protein interaction was investigated using co-immunoprecipitation and GST pull-down assays. In PANC-1 cells, TRAF1 restoration reversed NOP10 knockdown-induced suppression of NF-κB signalling and malignant phenotypes. The present study aimed to investigate the molecular mechanisms underlying NOP10-mediated pancreatic cancer progression, with particular emphasis on the TRAF1–NF-κB signalling pathway. The regulatory relationship and protein–protein interaction between NOP10 and TRAF1 were investigated, along with the role of TRAF1 in mediating NOP10-associated NF-κB signalling and malignant phenotypes.

Materials and Methods

Bioinformatics analysis

All clinical data analyzed in this study were obtained from publicly available databases. TCGA-PAAD expression and clinical follow-up data, together with GTEx normal pancreatic expression data, were retrieved from UCSC Xena (http://xena.ucsc.edu/). GEO datasets GSE15471, GSE32676, and GSE71989 were obtained from NCBI GEO (https://www.ncbi.nlm.nih.gov/geo/). Bioinformatics analyses were conducted using R version 4.2.1 and packages including Survival, survminer, pROC, and ggplot2. All datasets were publicly available and de-identified; therefore, ethics approval was not required.

NOP10 expression and prognostic analysis

NOP10 mRNA expression was compared between pancreatic cancer and normal pancreatic tissues using TCGA-PAAD and GTEx datasets. Paired samples in GSE15471 were analyzed using the paired Wilcoxon signed-rank test, whereas independent samples in GSE32676 and GSE71989 were compared using the Wilcoxon rank-sum test. For survival analysis, TCGA-PAAD patients were stratified into NOP10-high and NOP10-low groups based on median NOP10 expression. Overall survival (OS) was evaluated using the Kaplan–Meier method and log-rank test, with survival curves generated using the R packages survminer and Survival.

Correlation and gene set enrichment analysis

Pearson correlation analysis was performed to assess the relationship between NOP10 and TRAF1 mRNA expression in TCGA-PAAD. Gene set enrichment analysis (GSEA) was conducted using Hallmark gene sets after stratifying tumors according to NOP10 expression. Normalized enrichment scores (NES) and false discovery rates (FDR q) were reported. GSEA and related analyses were performed in R 4.2.1 using the clusterProfiler and fgsea packages.

Cell culture

Human pancreatic cancer cell lines PANC-1 and 8988T and the normal human pancreatic ductal epithelial cell line HPNE were obtained from the Cell Bank of the Chinese Academy of Sciences (Shanghai, China). All cell lines were maintained in DMEM supplemented with 10% fetal bovine serum (FBS) and 100 U/mL penicillin/streptomycin at 37°C in a humidified incubator containing 5% CO_2.

siRNA interference and plasmid transfection

Two siRNAs targeting NOP10 (si-NOP10#1 and si-NOP10#2) and a scrambled negative control (si-NC) were synthesized by RiboBio (Guangzhou, China), with sequences provided in Table S1. The TRAF1

overexpression plasmid and Flag-NOP10 and HA-TRAF1 plasmids for exogenous co-immunoprecipitation were custom-constructed by Beijing Maijin. Cell transfection was performed using Lipofectamine 3000 (Invitrogen) according to the manufacturer's instructions. Cells were harvested 48 h post-transfection. Rescue experiments were conducted exclusively in PANC-1 cells using three experimental groups: si-NC+Vector, si-NOP10 + Vector, and si-NOP10 + TRAF1.

RNA extraction and quantitative real-time PCR

Total RNA was isolated using TRIzol (Vazyme, China) and quantified by spectrophotometer. Complementary DNA was synthesized using the HiScript II Q RT SuperMix for qPCR kit (Vazyme, China). Quantitative real-time PCR was performed using a LightCycler 96 (Roche, Switzerland) with SYBR Green (Vazyme, China). Primer sequences are provided in Table S1. β-actin served as the internal reference, and relative gene expression was calculated using the $2^{-\Delta\Delta Ct}$ method.

Western blotting

Western blotting
Cells were lysed in RIPA buffer supplemented with PMSF and phosphatase inhibitors, followed by boiling in SDS loading buffer. Routine protein detection was performed using 15% SDS-PAGE and a low-molecular-weight prestained protein marker (Thermo Fisher Scientific) to verify NOP10 migration (~ 8 kDa). For co-immunoprecipitation and GST pull-down analyses, a 10% PAGE rapid preparation kit (Epizyme PG122) and Servicebio prestained Protein Marker II (G2058-250UL) were used. Proteins were transferred onto PVDF membranes (0.22 μm for NOP10), blocked with 5% skimmed milk, and incubated with primary antibodies overnight at 4°C, followed by HRP-conjugated secondary antibodies for 1 h at room temperature. Protein bands were visualized using ECL.

The primary antibodies included anti-NOP10 (Abcam ab133726, 1:1000), anti-TRAF1 (Abcam ab300075, 1:1000), anti-p65 (D14E12, CST #8242, 1:1000), anti-p-p65 (Ser536, 93H1, CST #3033, 1:1000), anti-p50 (D4P4D, CST #13586, 1:1000), anti-IκBα (44D4, CST #4812, 1:1000), and anti-GAPDH (14C10, CST #2118, 1:1000). All target-protein primary antibodies were rabbit-derived and detected using an HRP-conjugated anti-rabbit IgG secondary antibody. For exogenous co-immunoprecipitation, mouse anti-Flag (Proteintech 66008-4-Ig) and rabbit anti-HA (Proteintech 51064-2-AP) antibodies were used, followed by the corresponding anti-mouse or anti-rabbit secondary antibodies. TRAF1 and p50 were analyzed on separate membranes. GAPDH served as the loading control, while IκBα (~ 40 kDa) was resolved separately from GAPDH (~ 37 kDa). Band intensities were quantified using ImageJ. p-p65 levels were normalized to total p65, whereas other target proteins were normalized to GAPDH.

Immunohistochemistry

Paraffin-embedded pancreatic cancer and normal pancreatic tissue sections were deparaffinized in xylene, rehydrated through a graded alcohol series, treated with 3% hydrogen peroxide, and subjected to pressure-cooker-mediated antigen retrieval. Sections were incubated with anti-NOP10 primary antibody (Abcam, Cambridge, UK; ab133726) overnight at 4°C, followed by HRP-conjugated secondary antibody incubation for 1 h at room temperature. Immunoreactivity was visualized using 3,3'-diaminobenzidine tetrahydrochloride (DAB), followed by haematoxylin counterstaining. Representative images were acquired at original magnifications of 70× (scale bar, 400 μm) and 300× (scale bar, 50 μm).

RNA sequencing and data analysis

Transcriptomic sequencing was conducted using NOP10-knockdown and control cells comprising six groups: PANC1KD1, PANC1KD2, PANC1_NC, T8988KD1, T8988KD2, and T8988_NC, with three biological replicates per group (18 samples in total). Sequencing was performed by Hangzhou Guangke Ande Biotechnology Co., Ltd. (project no. FWGN20255328) using the Illumina NovaSeq 6000 platform. A total of 125.58 Gb of clean data were generated, with ≥ 6.16 Gb per sample and Q30 values ≥ 95.61%. Clean reads were mapped to the Homo sapiens GRCh38 reference genome (release-109) using HISAT2 (Kim et al. 2019), yielding alignment rates of 96.78% – 97.53%. Gene expression levels were quantified using featureCounts (Liao et al. 2014). Differential expression analysis was performed using DESeq2 (Love et al. 2014), with |FoldChange| > 1.5 and padj < 0.05 as the significance thresholds. DEGs shared between the two siRNAs within each cell line were identified, followed by intersection analysis across both cell lines. GO, KEGG, and Reactome enrichment analyses were performed on the common DEGs using clusterProfiler (Yu et al. 2012). GSEA was conducted using the complete ranked gene list, with NES and adjusted p-values reported.

Co-immunoprecipitation (Co-IP)

Flag-NOP10 and HA-TRAF1 plasmids (custom-constructed by Beijing Maijin) were co-transfected into 293T cells cultured in 6-well plates using Lipofectamine 3000 (Invitrogen), with 0.25 μg total DNA. After 4–6 h, the transfection medium was replaced with complete medium, and cells were harvested 24 h post-transfection. Cells were washed with ice-cold PBS and lysed in buffer containing 25 mM Tris-HCl, 150 mM NaCl, 1 mM EDTA, 1% NP-40, 1 mM PMSF, and protease/phosphatase inhibitors. Lysates were centrifuged at 14,000 × g for 15 min at 4°C. For each 1 mL of total protein lysate, 40 μL of 50% Protein A/G agarose beads were used for pre-clearing for 10 min at 4°C, followed by overnight incubation at 4°C with anti-HA (Proteintech 51064-2-AP) or anti-Flag (Proteintech 66008-4-Ig) antibodies. Immune complexes were captured using 100 μL of Protein A/G agarose beads, washed three times with cold RIPA buffer or PBS, and eluted by boiling in protein loading buffer. Eluted proteins and whole-cell lysate (WCL) inputs were analyzed by western blotting. Forward co-IP involved anti-HA immunoprecipitation followed by Flag immunoblotting, whereas reverse co-IP involved anti-Flag immunoprecipitation followed by HA immunoblotting. Interaction specificity was assessed through reciprocal co-immunoprecipitation with corresponding WCL inputs and further validated by GST pull-down using GST alone as a negative control. Experiments were independently performed three times (n = 3).

GST pull-down

GST pull-down assays were performed using a commercial kit (Solarbio, PC4400). GST-tagged bait protein (GST-NOP10), His-tagged prey protein (His-TRAF1), and GST control protein were custom-produced by Anhui General Biotech. GST-NOP10 and GST were expressed in E. coli, lysed by ultrasonication in protease inhibitor-supplemented lysis buffer, and centrifuged at 12,000 × g for 15 min at 4°C. Bait-protein inputs were retained for subsequent analysis. Glutathione-agarose resin was washed, equilibrated with ice-cold PBS, and prepared as a 50% slurry. For experimental and control conditions, 90 µL of 50% resin slurry was incubated with 20 µg of GST-NOP10 or GST, respectively, at 4°C for 1–2 h, followed by three washes with wash buffer. His-TRAF1 lysate was subsequently added to the resin and incubated for 3 h at room temperature or overnight at 4°C. Following centrifugation, the resin was washed three times and bound proteins were eluted using elution buffer. Eluates were analyzed by western blotting using anti-GST and anti-His antibodies. Input proteins (GST, GST-NOP10, and His-TRAF1) were analyzed to verify protein loading, with GST alone serving as the negative control. Experiments were independently performed three times (n = 3).

Functional assays

CCK-8 assay

Cells were seeded at a density of 2×10^3 cells per well in 96-well plates and cultured for 5 days. CCK-8 reagent (10 µL/well) was added daily, followed by incubation in the dark for 2 h. Absorbance was measured at 450 nm using a Multiskan FC microplate reader (Thermo Fisher Scientific).

Colony formation assay

Cells were seeded at 1000 cells per well in 6-well plates and cultured for 10–14 days. Colonies were fixed with methanol, stained with crystal violet, photographed, and counted.

Wound healing assay: Cells were seeded at 8×10^5 cells per well in 6-well plates. Upon reaching 100% confluence, monolayers were scratched using a 200 µL pipette tip, washed with PBS, and maintained in basal medium. Images were captured at 0 and 24 h, and wound closure was quantified using ImageJ. The remaining wound area was calculated as follows: remaining wound area (%) = (24 h wound area/0 h wound area) × 100%.

Transwell invasion assay

The upper chambers were pre-coated with Matrigel (BD Bioscience Pharmingen). Cells (2×10^4 per well) were suspended in 200 µL of serum-free medium and seeded into the upper chambers, while 600 µL of complete medium containing 10% FBS was added to the lower chambers. After 24 h, non-invading cells were removed from the upper membrane surface using cotton swabs. Invading cells were stained with 0.1% crystal violet for 30 min and counted.

Statistical analysis

Statistical analyses were performed using GraphPad Prism (version 9.0), SPSS (version 25.0), and R (version 4.2.1). Quantitative data are expressed as mean ± SD, and all experiments were independently repeated at least three times. Paired comparisons were performed using the paired t-test or Wilcoxon test, while unpaired comparisons were assessed using the t-test or Wilcoxon test. Multiple-group comparisons were conducted using one-way ANOVA, followed by Tukey's or Dunnett's post-hoc test. Survival analysis was performed using the Kaplan–Meier method and log-rank test, while correlations were evaluated using Pearson's correlation coefficient. All statistical tests were two-sided, with $p < 0.05$ considered statistically significant (*$p < 0.05$, **$p < 0.01$, ***$p < 0.001$, ****$p < 0.0001$).

Ethics statement

This study was approved by the Ethics Committee of Huai'an Second People's Hospital (approval no. HEYLL2023168), and written informed consent was obtained from all participants. Publicly available, de-identified datasets from TCGA, GTEx, and GEO were also analyzed. The *in vivo* findings referenced from our previously published study (Dou *et al.*, BMC Cancer 2024) were covered by the animal ethics approval granted by Nanjing Medical University (approval no. IACUC-1903002).

Results

NOP10 is upregulated in pancreatic cancer and associated with poor prognosis

NOP10 expression was initially assessed in pancreatic cancer and normal pancreatic tissues using publicly available transcriptomic datasets. Analysis of TCGA-PAAD, with normal pancreatic tissues from GTEx serving as controls, revealed significantly elevated NOP10 expression in pancreatic cancer tissues ($p < 2 \times 10^{-16}$; Fig. 1A). A similar expression pattern was observed in paired tumor and adjacent normal tissue samples from GSE15471, where NOP10 expression was significantly higher in tumor tissues (paired test, $p = 2.9 \times 10^{-7}$; Fig. 1B). This was further supported by two independent GEO datasets, GSE32676 ($p = 0.0032$) and GSE71989 ($p = 0.0012$), both of which showed significantly increased NOP10 expression in pancreatic cancer tissues, as assessed using the Wilcoxon rank-sum test (Fig. 1C).

Consistent with the transcriptomic findings, qRT-PCR and Western blot analyses revealed significantly higher NOP10 mRNA and protein expression in PANC-1 and 8988T cells than in HPNE cells (Fig. 1G, H). Immunohistochemical analysis of tissue samples from our cohort further confirmed elevated NOP10 protein expression in pancreatic cancer tissues relative to adjacent normal pancreatic tissues (Fig. 1E, F). These observations are consistent with the previously published findings of Dou *et al.* (BMC Cancer, 2024). This study further validates NOP10 upregulation across independent GEO cohorts and investigates its downstream molecular

mechanisms in pancreatic cancer. To assess the prognostic relevance of NOP10 expression, patients in the TCGA-PAAD cohort were stratified into NOP10-high (n = 89) and NOP10-low (n = 88) groups based on the median expression level. Kaplan–Meier survival analysis revealed significantly shorter OS in patients with high NOP10 expression than in those with low expression (log-rank $p = 0.017$; Fig. 1D). These results indicate that elevated NOP10 expression is associated with unfavorable clinical outcomes in pancreatic cancer.

NOP10 promotes the malignant phenotypes of pancreatic cancer cells

To investigate the biological role of NOP10, two independent siRNAs were used to knock down NOP10, while plasmid transfection was performed to overexpress NOP10 in PANC-1 and 8988T cells. Knockdown and overexpression efficiencies were confirmed by qRT-PCR and Western blot analyses (Fig. 2A, G). NOP10 knockdown significantly inhibited cell proliferation, as indicated by reduced CCK-8 growth curves ($p < 0.01$) and decreased colony formation. It also impaired cell migration and invasion, as evidenced by delayed wound closure and fewer invaded cells in the Transwell assay (Fig. 2B–E). In comparison, NOP10 overexpression significantly increased colony formation and cell migration (Fig. 2F, H). These gain- and loss-of-function experiments indicate that NOP10 promotes the proliferation, migration, and invasion of pancreatic cancer cells.

Transcriptomic screening identifies TRAF1 as a downstream target of NOP10.

To identify downstream effectors regulated by NOP10, RNA sequencing was performed in PANC-1 and 8988T cells following knockdown with two independent siRNAs (si-NOP10#1 and si-NOP10#2), using si-NC as the control (three biological replicates per group). Differential expression analysis ($|FoldChange| > 1.5$, $padj < 0.05$) identified 1243 (940 upregulated/303 downregulated) and 280 (84/196) DEGs in the two PANC-1 comparisons, and 519 (202/317) and 699 (225/474) in the two 8988T comparisons (Fig. 3A). Intersection analysis of the two siRNAs within each cell line, followed by comparison between the two cell lines, identified 20 common DEGs, including TRAF1 and TNF (Fig. 3B; Table S1).

Pathway enrichment analysis revealed prominent changes in TNF/NF-κB-related signalling following NOP10 knockdown. KEGG analysis identified significant enrichment of the TNF signalling pathway in both PANC-1 siRNA comparisons (adjusted $p = 5.7\times10^{-5}$ and 7.2×10^{-8}) and the NF-κB signalling pathway in the si-NOP10#2 comparisons (adjusted $p = 3.5\times10^{-3}$; Fig. 3C). GSEA further revealed significant downregulation of the TNF signalling pathway gene set across all four comparisons (NES < 0, adjusted < 0.05), while the NF-κB signalling pathway gene set was significantly downregulated in three comparisons (adjusted $p = 7.9\times10^{-3}$, 1.3×10^{-5}, and 2.3×10^{-4}; Fig. 3D). Reactome analysis of the 20 common genes identified significant enrichment of TNFR1-induced NF-κB signalling (adjusted $p = 0.037$). GO analysis also revealed enrichment of TNF-mediated signalling and positive regulation of NF-κB transcription factor activity (Table S2). TRAF1 was selected as a candidate downstream target of NOP10 based on its role as an adaptor protein in TNFR1/NF-κB signalling.

The regulatory relationship between NOP10 and TRAF1 was further investigated. Transcriptomic analysis revealed significant downregulation of TRAF1 across all four comparisons (log2FC ranging from − 0.64 to − 1.43; adjusted *p* ranging from 2.5×10^{-2} to 1.8×10^{-8}; Fig. 3E; Table S1). qRT-PCR and IGV visualization confirmed reduced TRAF1 mRNA expression following NOP10 knockdown. Western blot analysis further showed decreased TRAF1 protein expression following NOP10 knockdown, whereas NOP10 overexpression increased TRAF1 protein levels (Fig. 3F, G). Analysis of TCGA-PAAD data revealed a positive correlation between NOP10 and TRAF1 mRNA expression (Pearson r = 0.233, *p* = 0.0018; Fig. 3H). GSEA also identified significant enrichment of TNFα/NF-κB signalling in NOP10-high tumors (NES = 2.37, FDR q = 5.6×10^{-10}; Additional file 1). These results indicate that NOP10 positively regulates TRAF1 expression and is associated with NF-κB pathway activity in clinical samples.

NOP10 directly interacts with TRAF1

NOP10 knockdown was accompanied by decreased TRAF1 protein expression; therefore, we next investigated whether the two proteins physically interact. Following co-transfection of Flag-NOP10 and HA-TRAF1, immunoprecipitation with anti-HA pulled down Flag-NOP10, whereas immunoprecipitation with anti-Flag pulled down HA-TRAF1. WCL inputs confirmed the expression of both tagged proteins (Fig. 4B). To determine whether this interaction was direct, a GST pull-down assay was performed. GST-NOP10 specifically retained His-TRAF1, whereas GST alone did not, and input samples confirmed the presence of GST, GST-NOP10, and His-TRAF1 (Fig. 4A). These results indicate a direct *in vitro* interaction between NOP10 and TRAF1.

Restoration of TRAF1 rescues NF-κB signalling and malignant phenotypes upon NOP10 knockdown.

To investigate whether TRAF1 mediates the biological effects of NOP10, a TRAF1 overexpression plasmid was co-transfected into si-NOP10-treated PANC-1 cells, generating three groups: si-NC+Vector, si-NOP10 + Vector, and si-NOP10 + TRAF1. Western blot analysis confirmed the restoration of TRAF1 expression in the si-NOP10 + TRAF1 group, accompanied by increased p-p65 and p50 levels and reduced IκBα expression, indicating reactivation of NF-κB signalling (Fig. 4C). TRAF1 restoration significantly reversed the inhibitory effects of NOP10 knockdown on proliferation, wound healing, colony formation, and Transwell invasion (Fig. 4D–G). No significant differences were observed between the si-NOP10 + TRAF1 and si-NC+Vector groups. These results suggest that TRAF1 mediates NOP10-associated NF-κB signalling and malignant phenotypes in pancreatic cancer cells.

Discussion

Our previous study established that NOP10 is overexpressed in pancreatic cancer, predicts poor prognosis, and promotes malignant phenotypes and subcutaneous tumor growth (Dou et al. 2024); however, the downstream mechanism remained undefined. In the present study, transcriptomic profiling identified TRAF1 as a NOP10-regulated gene, reciprocal co-immunoprecipitation and GST pull-down assays confirmed a direct NOP10–TRAF1 interaction, and rescue experiments showed that TRAF1 restoration reverses the suppression of NF-κB signalling and malignant phenotypes induced by NOP10

knockdown. These results establish the NOP10–TRAF1–NF-κB axis as a previously unrecognized oncogenic signalling pathway in pancreatic cancer.

Accumulating evidence indicates that snoRNAs and their associated snoRNP components are frequently deregulated in cancer and contribute to malignant phenotypes (Ye et al. 2025; Chauhan et al. 2024). Several snoRNP components, including RRP9, NOP56, and fibrillarin, sustain cancer cell proliferation, migration, or oncogenic translation through distinct mechanisms (Li et al. 2025a; Park et al. 2026; Groza et al. 2026; Kellett et al. 2025; Zhang et al. 2026). Our findings extend these observations by showing that NOP10 exerts its oncogenic function through a defined signalling route—direct TRAF1 binding and subsequent NF-κB activation—rather than solely through its canonical roles in pseudouridylation and ribosome assembly. This suggests that snoRNP components can support malignancy by coupling RNA processing to inflammatory signalling.

TRAF1 serves as an adaptor within the TNFR1 signalling complex, where it supports the K63-linked ubiquitination events required for IKK activation (Jang et al. 2024; He et al. 2026). Consistent with its pro-tumorigenic functions in gastric cancer and osteosarcoma (Zhang et al. 2025; Wang et al. 2025), our data identify TRAF1 as a downstream oncogenic effector of NOP10 in pancreatic cancer cells. The direct NOP10–TRAF1 interaction may enhance TRAF1 availability within the TNFR1 complex, thereby promoting IκBα degradation and p65/p50 activation, which is consistent with the restored p-p65 and p50 levels and reduced IκBα observed upon TRAF1 restoration. In addition, NOP10 positively regulates TRAF1 at the mRNA level, raising the possibility of a feed-forward loop in which NOP10 sustains both TRAF1 expression and TRAF1-dependent NF-κB activity. Because CHX chase and related stability assays were not performed, the precise post-translational mechanism by which NOP10 maintains TRAF1 protein abundance remains to be determined; nonetheless, these data establish a functional requirement for TRAF1 in NOP10-driven NF-κB activation.

NF-κB signalling is persistently activated in pancreatic cancer and underlies cell growth, survival, and drug resistance (Li et al. 2026; Zhou et al. 2026; Chen et al. 2025), positioning the NOP10–TRAF1–NF-κB axis as a candidate therapeutic target. Direct NF-κB inhibition has been limited by systemic toxicity and poor selectivity, whereas disrupting the upstream NOP10–TRAF1 interface may attenuate tumor-specific NF-κB activity. The emerging anticancer potential of targeting snoRNP components and ribosome biogenesis (Kellett et al. 2025; Zhang et al. 2026) further suggests that NOP10 may act as a dual-purpose target, simultaneously impairing oncogenic translation and TRAF1-mediated NF-κB activation. Together with the expanding arsenal of experimental therapies for pancreatic cancer, including KRAS-directed agents and immunotherapies (Fan et al. 2025; Qin et al. 2024; Chen et al. 2026; Tonini and Zanni 2025; Fivaz et al. 2025; Yi et al. 2025; Mahat et al. 2025; Mosalem et al. 2025), these findings provide a molecular framework for exploring the NOP10–TRAF1 interface as a therapeutic node.

This study has several limitations. First, the functional and mechanistic evidence was derived primarily from in vitro experiments, and in vivo tumor-growth data were obtained from our previously published work (Dou et al. 2024). Second, rescue experiments were performed exclusively in PANC-1 cells, so

validation in additional pancreatic cancer models is needed. Third, the NOP10–TRAF1 interaction was demonstrated by exogenous co-immunoprecipitation and GST pull-down, whereas endogenous co-immunoprecipitation and immunofluorescence co-localization were not performed. Fourth, CHX chase, NF-κB nuclear translocation, and luciferase reporter assays were not conducted, leaving the mechanisms underlying TRAF1 protein regulation and NF-κB activation incompletely characterized. Fifth, the transcriptomic analysis relied on transient siRNA-mediated knockdown, and the TCGA-PAAD correlation between NOP10 and TRAF1 was modest (r = 0.233) with inter-cohort heterogeneity across the GEO datasets. Future studies incorporating endogenous interaction assays, RIP/CLIP, protein stability analyses, in vivo mechanistic validation, and clinical sample validation will be necessary to fully establish the pathophysiological significance of the NOP10–TRAF1–NF-κB axis.

Conclusions

In conclusion, NOP10 is overexpressed in pancreatic cancer and is associated with poor prognosis. NOP10 directly interacts with TRAF1 and activates NF-κB signalling in a TRAF1-dependent manner, promoting the proliferation, migration, and invasion of pancreatic cancer cells; restoration of TRAF1 reverses these effects upon NOP10 knockdown. These results establish the NOP10–TRAF1–NF-κB pathway as a novel oncogenic signalling pathway and a potential therapeutic target in pancreatic cancer.

Figure legends

Additional file 1

Table S1, 20 common DEGs; Table S2, GO and Reactome enrichment analyses; and Fig. S1, GSEA of TNFα/NF-κB signalling in TCGA-PAAD tumors with high NOP10 expression.

Declarations

Competing Interests:

The authors declare no competing interests.

Ethics approval:

This study was approved by the Ethics Committee of Huai'an Second People's Hospital (approval no. HEYLL2023168).

Consent to participate:

Written informed consent was obtained from all participants.

Consent for publication:

Not applicable.

Funding:

This work was supported by the Postgraduate Research & Practice Innovation Program of Jiangsu Province (Grant No. 26CXJH5320), the Natural Science Research Programme of Huai'an (Grant Nos. HAP202501 and HAB2025052), and the Huai'an Health Commission Research Project (Grant No. HAWJ2024016).

Author Contribution

J.D., J.F., and X.W. contributed equally to this work. J.D., J.F., and X.W. wrote the main manuscript text and prepared the figures. J.D., J.F., X.W., M.L., and S.J. performed the experiments and bioinformatics analyses. H.Z. and X.Z. conceived and designed the study, supervised the project, and critically revised the manuscript. All authors reviewed the manuscript and approved the final version.

Acknowledgements:

The authors acknowledge Hangzhou Guangke Ande Biotechnology Co., Ltd. for providing RNA sequencing and bioinformatics support (Project No. FWGN20255328).

Data Availability:

The datasets analyzed in this study are publicly available through TCGA (https://portal.gdc.cancer.gov/), GTEx (https://gtexportal.org/), and GEO (GSE15471, GSE32676, and GSE71989). The RNA-seq data generated during this study are available from the corresponding author upon reasonable request.

References

1. Blackford AL, Canto MI, Dbouk M et al (2024) Pancreatic Cancer Surveillance and Survival of High-Risk Individuals. JAMA Oncol 10:1087–1096
2. Cao M, Peng W, Cheng B et al (2025) PPY-Induced iCAFs Cultivate an Immunosuppressive Microenvironment in Pancreatic Cancer. Adv Sci (Weinh) 12:e2413432
3. Chauhan W, Sudharshan Sj, Kafle S et al (2024) SnoRNAs: Exploring Their Implication in Human Diseases. Int J Mol Sci 25:7202

4. Chen K, Ma Y, Huang L et al (2026) Complement-secreting CAFs are associated with better prognosis in pancreatic cancer: single-cell multiomics. Gut 75:1367–1382
5. Chen Q, Xu Y, Wang Y et al (2025) Bacteria and tumor debris induced pancreatic cancer progression via the NF-κB signaling pathway. Cancer Lett 632:217964
6. Ding J, Xie Y, Liu Z et al (2025) Hypoxic and Acidic Tumor Microenvironment-Driven AVL9 Promotes Chemoresistance of Pancreatic Ductal Adenocarcinoma via the AVL9-IκBα-SKP1 Complex. Gastroenterology 168:539–555e5
7. Dou J, Hu W, Zhang X et al (2024) NOP10 predicts poor prognosis and promotes pancreatic cancer progression. BMC Cancer 24:1394
8. Fan X, Dai Y, Mo C et al (2025) TRIM21 Promotes Tumor Growth and Gemcitabine Resistance in Pancreatic Cancer by Inhibiting EPHX1-Mediated Arachidonic Acid Metabolism. Adv Sci (Weinh) 12:e2413674
9. Fivaz M, Bornand A, Corro C et al (2025) Actionable mutations in pancreatic cancer: where targeted therapies are making a difference. BMJ Open Gastroenterol 12:e001925
10. Gadeock S, Girish N, Liu CY et al (2026) Tumor Necrosis Factor Receptor 1 Regulates Colonic Mesenchymal Cell Diversity and the Epithelial Stem Cell Niche. Cell Mol Gastroenterol Hepatol 20:101856
11. Ghanim GE, Sekne Z, Balch S et al (2024) 2.7 Å cryo-EM structure of human telomerase H/ACA ribonucleoprotein. Nat Commun 15:746
12. Groza P, Kumari K, Esteva-Socias M et al (2026) Fibrillarin-dependent 2'-O-methylation modulates RPS28 ribosome incorporation and oncogenic translation. Cancer Lett 639:218124
13. He J, Huang X, Xing D et al (2026) UBE2B Drives NF-κB Signaling and Gastric Cancer Progression through BIRC2-Mediated K63-Linked Ubiquitination of TRAF1. Mol Cancer Res 24:487–503
14. Jamal MH, Khan MN (2025) Developments in pancreatic cancer emerging therapies, diagnostic methods, and epidemiology. Pathol Res Pract 271:156012
15. Jang H, Kim S, Kim DY et al (2024) TRAF1 from a Structural Perspective. Biomolecules 14:510
16. Jenkins BH, Tracy I, Rodrigues MFSD et al (2025) Single cell and spatial analysis of immune-hot and immune-cold tumours identifies fibroblast subtypes associated with distinct immunological niches and positive immunotherapy response. Mol Cancer 24:3
17. Kellett MD, Sharma V, Sherlock ME et al (2025) Focal adhesion kinase promotes ribosome biogenesis to drive advanced thyroid cancer cell growth and survival. Front Oncol 15:1252544
18. Kim D, Paggi JM, Park C et al (2019) Graph-based genome alignment and genotyping with HISAT2 and HISAT-genotype. Nat Biotechnol 37:907–915
19. Li B, Shen L, Huang H et al (2025a) snoRNP RRP9 Promotes Prostate Cancer Cell Proliferation and Migration via SQSTM1. Adv Biol (Weinh) 9:e00182
20. Li C, Fu K, Wu F et al (2026) FBXL8 Stabilizes IκBα and Negatively Regulated NF-κB Activation to Suppress Pancreatic Cancer Progression. Int J Biol Sci 22:1461–1479

21. Li Y, Tang S, Wang H et al (2025b) A pancreatic cancer organoid biobank links multi-omics signatures to therapeutic response and clinical evaluation of statin combination therapy. Cell Stem Cell 32:1369–1389e14
22. Liao Y, Smyth GK, Shi W (2014) featureCounts: an efficient general purpose program for assigning sequence reads to genomic features. Bioinformatics 30:923–930
23. Love MI, Huber W, Anders S (2014) Moderated estimation of fold change and dispersion for RNA-seq data with DESeq2. Genome Biol 15:550
24. Mahat DB, Kumra H, Castro SA et al (2025) Mutant p53 exploits enhancers to elevate immunosuppressive chemokine expression and impair immune checkpoint inhibitors in pancreatic cancer. Immunity 58:1688–1705e9
25. Mannucci A, Goel A (2026) Advances in pancreatic cancer early diagnosis, prevention, and treatment: The past, the present, and the future. CA Cancer J Clin 76:e70035
26. Mosalem OM, Abdelhakeem A, Abdel-Razeq NH et al (2025) Pancreatic ductal adenocarcinoma (PDAC): clinical progress in the last five years. Expert Opin Investig Drugs 34:149–160
27. Panwar HS, Vos TJ, Xie X et al (2025) Interprotomer communication and functional asymmetry in H/ACA snoRNPs. Proc Natl Acad Sci U S A 122:e2514683122
28. Park JE, Ahn CH, Sim DY et al (2026) NOP56 Drives Colorectal Cancer Progression by Modulating p53 Acetylation through SIRT1/p300. Int J Biol Sci 22:4537–4554
29. Qin Q, Yu R, Eriksson JE et al (2024) Cancer-associated fibroblasts in pancreatic ductal adenocarcinoma therapy: Challenges and opportunities. Cancer Lett 591:216859
30. Singhal A, Styers HC, Rub J et al (2024) A Classical Epithelial State Drives Acute Resistance to KRAS Inhibition in Pancreatic Cancer. Cancer Discov 14:2122–2134
31. Stoop TF, Javed AA, Oba A et al (2025) Pancreatic cancer. Lancet 405:1182–1202
32. Tang R, Jin L, Chen C et al (2026) Mapping cell type-resolved transcriptomic profiles to patient survival in pancreatic cancer. Cancer Cell 44:1623–1638e11
33. Tonini V, Zanni M (2025) Pancreatic cancer in 2025: Have we found a solution? World J Gastroenterol 31:111433
34. Wang Z, Fang Y, Yu Y et al (2025) ALKBH1-mediated N6-methyladenosine methylation of TRAF1 promotes osteosarcoma proliferation and metastasis. Am J Cancer Res 15:375–389
35. Yang D, Sun X, Wang H et al (2025) TREM2 Depletion in Pancreatic Cancer Elicits Pathogenic Inflammation and Accelerates Tumor Progression via Enriching IL-1β(+) Macrophages. Gastroenterology 168:1153–1169
36. Ye C, Yu X, Yan J et al (2025) Biological roles and potential clinical values of snoRNAs in Cancer. Int J Biol Macromol 328:147654
37. Yi S, Noh K, Kim H et al (2025) Advancing pancreatic cancer therapy by mesothelin-specific nanobody conjugation. Mol Cancer 24:124

38. Yu G, Wang LG, Han Y et al (2012) clusterProfiler: an R package for comparing biological themes among gene clusters. OMICS 16:284–287
39. Yuan L, Yao S, Qu N et al (2025) Helicobacter pylori VacA modulates TRAF1-mediated 4-1BB/NF-κB axis to induce host apoptosis and chronic inflammatory damage. Mol Med 31:317
40. Zhang M, Yuan L, Yang X et al (2025) TRAF1 promotes the progression of Helicobacter pylori-associated gastric cancer through EGFR/STAT/OAS signalling. Life Sci 373:123656
41. Zhang Z, Zhang M, Cao Z et al (2026) Fibrillarin: bridging ribosome biogenesis and apoptosis in cellular stress and disease. Apoptosis 31:11
42. Zhou S, Li Y, Wang C et al (2026) K11- and K29-ubiquitination-mediated nuclear translocation of glycolytic enzyme aldolase A promotes pancreatic cancer progression by NF-κB activation. Cell Death Differ 33:496–511

Figures

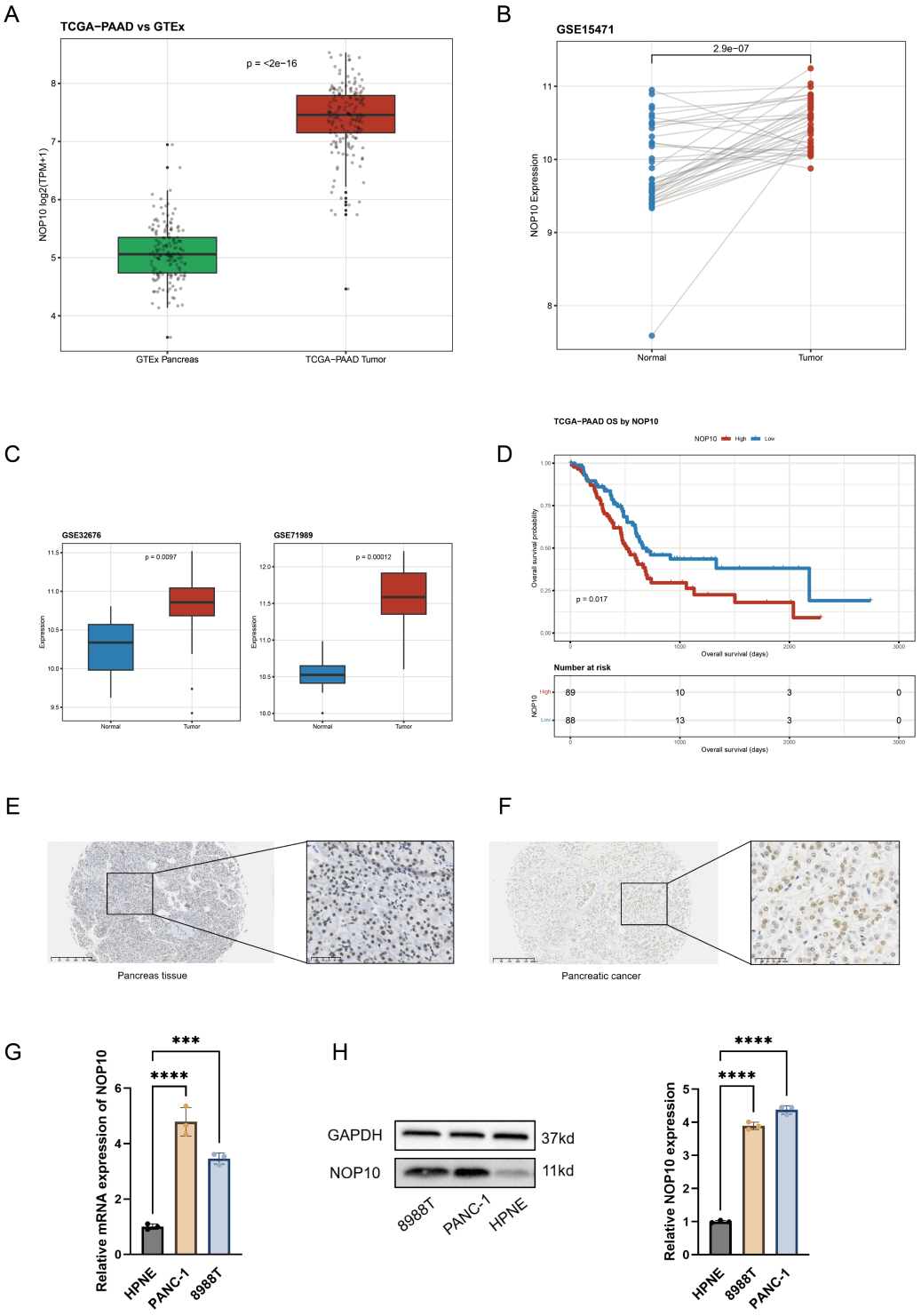

Figure 1

NOP10 is upregulated in pancreatic cancer and is associated with poor prognosis. (A) Comparison of NOP10 mRNA expression between pancreatic cancer tissues (TCGA-PAAD) and normal pancreatic tissues (GTEx) ($p < 2 \times 10^{-16}$). **(B)** Analysis of NOP10 expression in paired pancreatic cancer and adjacent normal tissues from GSE15471 (paired test, $p = 2.9 \times 10^{-7}$). **(C)** Assessment of NOP10 expression in GSE32676 ($p = 0.0032$) and GSE71989 ($p = 0.0012$) using the Wilcoxon rank-sum test. **(D)**

Kaplan–Meier analysis of OS in patients stratified into NOP10-high (n = 89) and NOP10-low (n = 88) expression groups in the TCGA-PAAD cohort (log-rank *p* = 0.017). **(E, F)** Representative immunohistochemical staining of NOP10 in adjacent normal pancreatic tissues (E) and pancreatic cancer tissues (F) at original magnifications of 70× (scale bar = 400 μm) and 300× (scale bar = 50 μm). **(G, H)** Comparison of NOP10 mRNA and protein expression levels in PANC-1 and 8988T cells relative to HPNE cells, as assessed by qRT-PCR (G) and Western blot analysis (H), respectively. Data are expressed as mean ± SD (n = 3 for G and H).

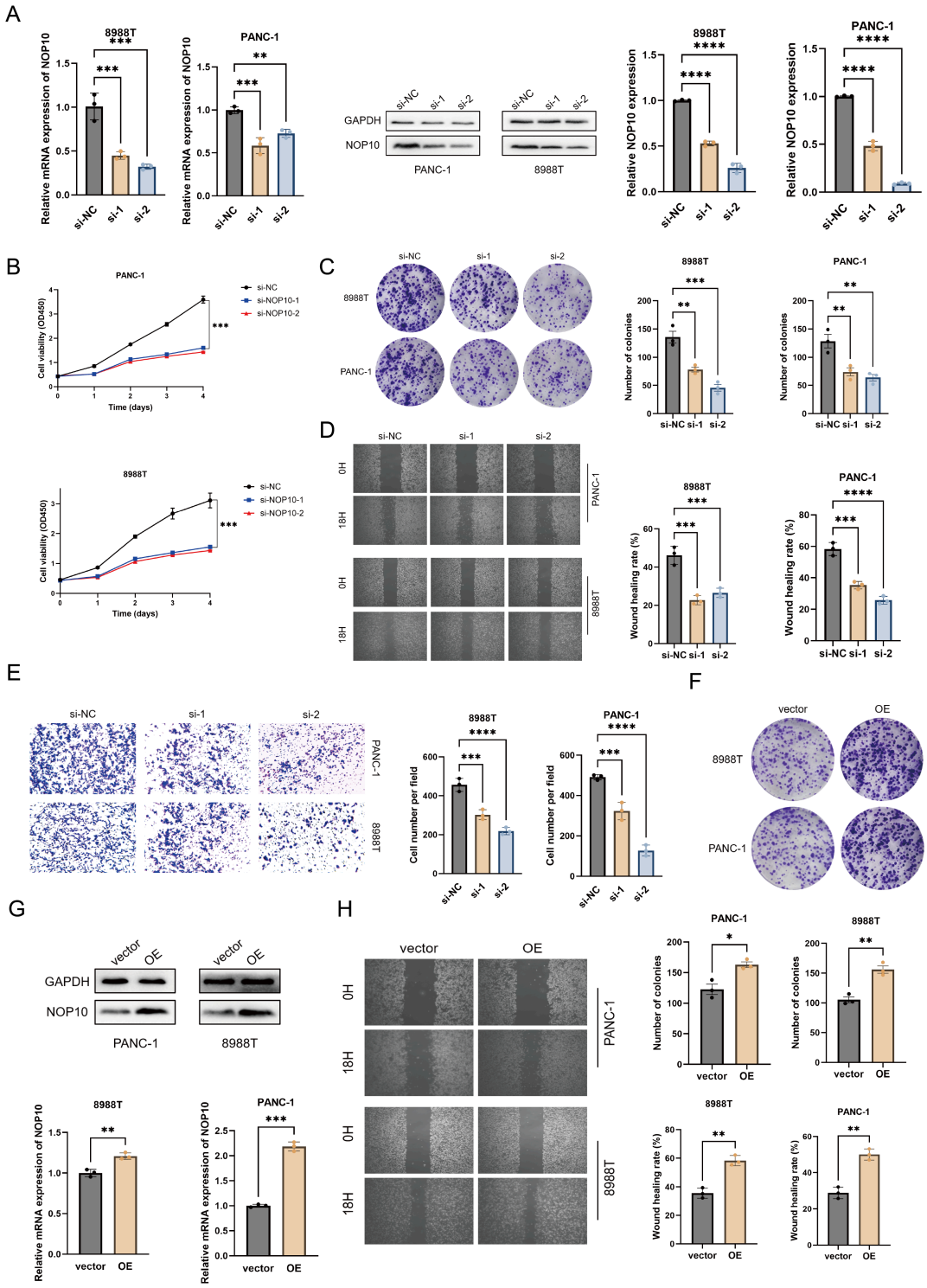

Figure 2

NOP10 promotes the proliferation, migration,and invasion of pancreatic cancer cells *in vitro*. (A) Evaluation of NOP10 knockdown efficiency in PANC-1 and 8988T cells by qRT-PCR and Western blot analyses, with densitometric quantification of protein expression. (B) CCK-8 assay showing reduced cell proliferation following NOP10 knockdown in PANC-1 and 8988T cells. (C) Colony formation assay demonstrating decreased clonogenic capacity upon NOP10 knockdown. (D)Wound healing assay showing impaired migratory capacity following NOP10 knockdown, with quantitative analysis of wound closure presented on the right. (E) Transwell invasion assay showing reduced invasive capacity following NOP10 knockdown, with quantification of invaded cells presented on the right. (F) Colony formation assay showing enhanced clonogenic capacity followingNOP10 overexpression, with quantitative colony counts presented on the right. (G) Evaluation of NOP10 overexpression efficiency in PANC-1 and 8988T cells by qRT-PCR and Western blot analyses. (H) Wound healing assay showing enhanced migratory capacity followingNOP10 overexpression, with quantitative analysis of wound closure presented on the right. Data are expressed as mean ± SD (n = 3). *$p < 0.05$, **$p < 0.01$, ***$p < 0.001$.

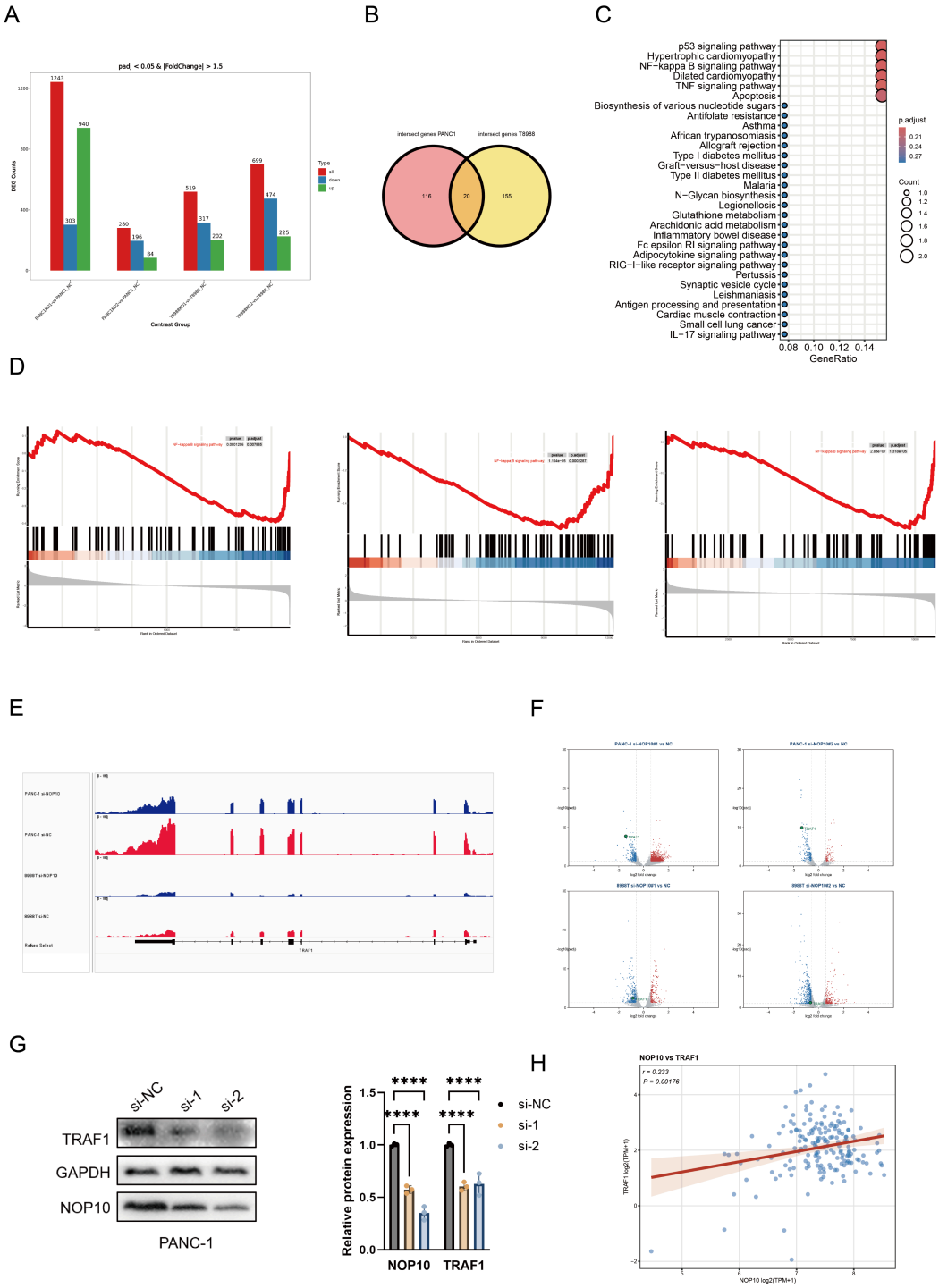

Figure 3

Transcriptomic profilingidentifies TRAF1 as a downstream target of NOP10. (A) Number of DEGs identified across the four siRNA-versus-control comparisons. (B)Venn diagram illustrating the 20 DEGs commonly identified across two pancreatic cancer cell lines following NOP10 knockdown with two independent siRNAs, including TRAF1 and TNF. (C)KEGG pathway enrichment analysis identifying significant enrichment of the TNF and NF-κB signalling pathways. (D)GSEA of the NF-κB signalling

pathway gene set (hsa04064) in NOP10-knockdown cells (PANC1KD1, PANC1KD2, and T8988KD1). (E) Volcano plots highlighting TRAF1 among the significantly downregulated genes following NOP10 knockdown. (F) qRT-PCR and IGV analyses validating the reduction in TRAF1 mRNA expression following NOP10 knockdown. (G) Western blot analysis ofTRAF1 protein expression following NOP10 knockdown and NOP10 overexpression. (H) Correlation analysis of NOP10 and TRAF1 mRNA expression in the TCGA-PAAD cohort (Pearson's r = 0.233, *p* = 0.0018).

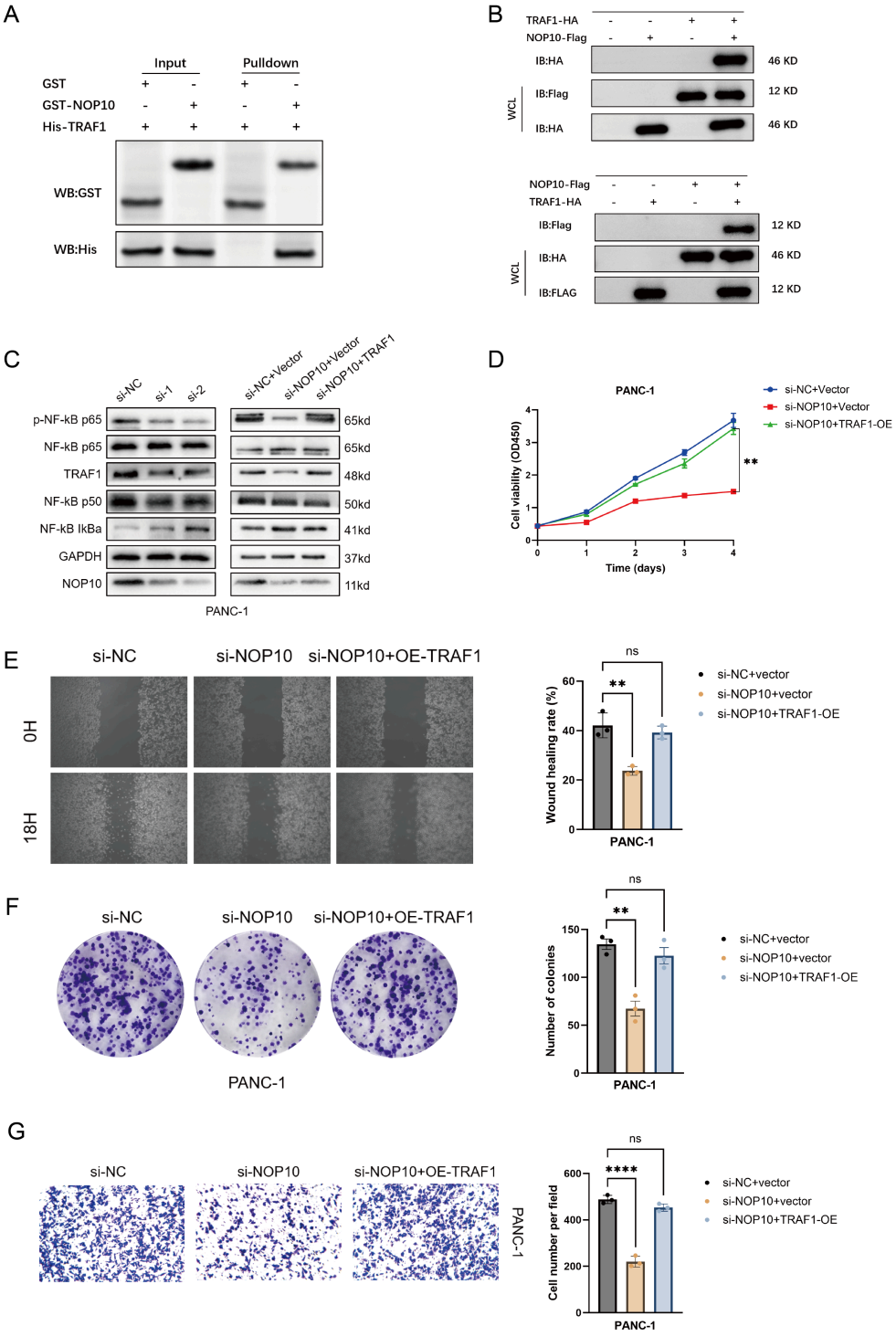

Figure 4

NOP10 directly interacts with TRAF1 and promotes pancreatic cancer cellproliferation, migration, and invasion through the TRAF1/NF-κB signalling axis. (A) GST pull-down assay confirming the direct *in vitro* interaction between recombinant GST-NOP10 and His-TRAF1. (B)Co-immunoprecipitation analysis validating the physical association between Flag-NOP10 and HA-TRAF1 in cells, with WCLincluded as inputcontrols. (C) Western blot analysis of NOP10, TRAF1, and NF-κB pathway-associated proteins following NOP10 knockdown and TRAF1 restoration in PANC-1 cells; GAPDH was used as the loading control. (D)CCK-8 assay showing that NOP10 knockdown suppresses PANC-1 cell proliferation, whereas TRAF1 overexpression significantly rescues this inhibitory effect. (E) Wound healing assay of the si-NC+Vector, si-NOP10+Vector, and si-NOP10+TRAF1 groups, with quantitative analysis of wound closure presented on the right. (F) Colony formation assay of the indicated groups, with quantitative colony counts shown on the right. (G)Transwell invasion assay of the indicated groups, with quantitative analysis of invaded cells presented on the right. Data represent at least three independent experiments and are expressed as mean ± SD. $^{**}p < 0.01$; ns, not significant.

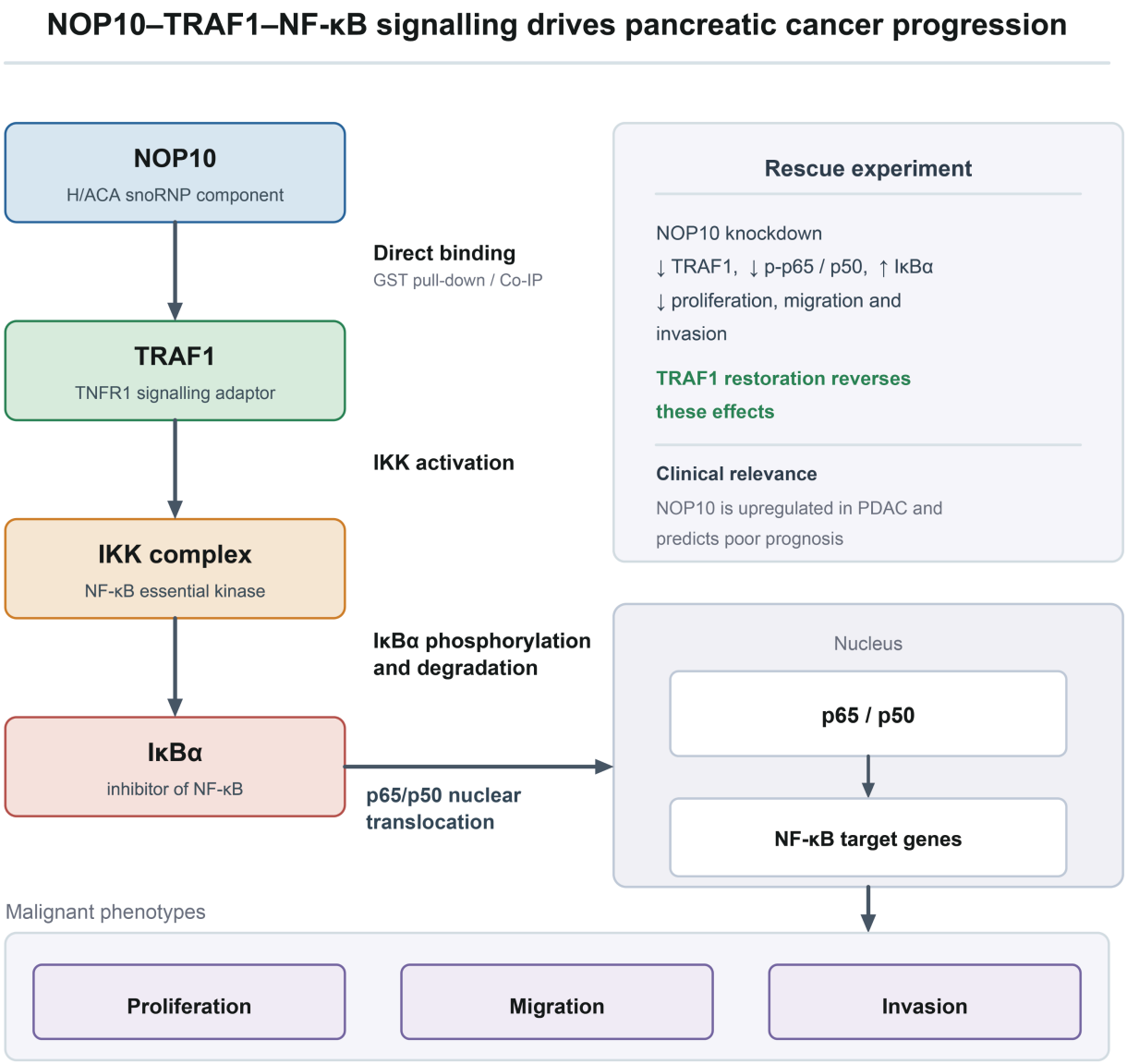

Figure 5

Schematic representationof the NOP10–TRAF1–NF-κB signalling pathwayin pancreatic cancer.NOP10 is upregulated in pancreatic cancer and directly interacts with TRAF1, leading to activation of the IKK complex and phosphorylation and degradation of IκBα. This process facilitates the nuclear translocation of p65/p50 dimers, resulting in the transcriptional activation of NF-κB target genes and promoting pancreatic cancer cell proliferation, migration, and invasion. NOP10 knockdown reduces TRAF1 expression and attenuates NF-κB signalling, thus suppressing these malignant phenotypes, whereas TRAF1 restoration counteracts the effects associated with NOP10 depletion.

Supplementary Files

This is a list of supplementary files associated with this preprint. Click to download.

- Fig.S1.pdf
- Supplementarymaterial.pdf